Pressurised CO2 Pipeline Rupture

Haroun Mahgerefteh* and Garfield Denton
Department of Chemical Engineering, University College London WC1E 7JE
Yuri Rykov, Keldysh Institute of Applied Mathematics, 125047, Moscow, Russia

Abstract

Outflow data using a validated CFD model for the hypothetical full bore rupture of a pressurised pipeline transporting CO2 are presented. For the sake of an example, the selected pipeline operating pressure of 117bara, 54km long and 0.42m dia. are the same as those for the main gas riser connecting the Piper Alpha to the MCP which ruptured during the Piper Alpha tragedy. Comparison of the CO2 discharge data with those for the actual Piper Alpha natural gas composition indicate significantly greater amount of CO2 released. Although both pipelines exhibit very similar depressurisation rates, almost 250,000kg of CO2 corresponding to only 3.7% of the total inventory is released in the first 300s following rupture. This compares with 125,000 kg of natural gas (9.7% of the total inventory) released for the same time duration. The temperature profile data indicate a significant drop in the temperature of CO2 at the rupture plane corresponding to solid discharge at – 62^{o}C and 4.1bara some 900s following pipeline failure. The combination of the massive amount of CO2 released in a relatively short period of time, the resulting dense cloud followed by solid discharge and its slow sublimation will pose a major challenge to safety practitioners when dealing with the hazards associated with the failure of pressurised CO2 pipelines.

*Corresponding author (h.mahgerefteh@ucl.ac.uk)

Introduction

It is now well established that increasing amounts of CO2 in the earth's atmosphere is leading to changes in the climate. Global use of fossil fuel which is the most significant source of CO2 currently results in an annual emission of 32Gt of CO_2 to the atmosphere. The concentration now stands at about 375ppm by volume compared with a stable, pre-industrial level of around 280ppm, maintained for at least the last 6,000 years (UK Department of Trade and Industry report, 2002). UK is responsible for 2.3% of CO2 emissions, despite the fact that it accounts for only 0.8% of the world population. It is the 6th largest producer of CO2 per capita amongst the world (World Population Prospects, 2002).

In order to stabilise CO2 concentrations or reduce them, global emissions of CO2 would need to decrease dramatically.

Given this a portfolio of approaches is needed to drive CO2 emissions down without impeding economic growth. For fossil fuels, this will mean ultimately the capture, transportation and long terms sequestration (CCS) of CO2.

Bulk gaseous transport of CO2 may be undertaken by tanker or pipeline. In view of the large volumes involved, pressurised pipelines are considered to be the most practical, and possibly the only option for many fossil fired generation plant. This has significant implications for the UK since more than 70% of its electricity is fossil fuel power generated (Energy Review, 2002). Additionally, given that most electricity generation plants are built close to energy consumers, the number of people potentially exposed to risks from CO2 transportation facilities will be greater than the corresponding number exposed to potential risks from CO2 capture and storage facilities.

Ironically (in line with its abbreviation), CCS and related legislation generally focus on the Capture and Sequestration of CO2 and not on its Transportation. This is despite Intergovernmental Panel on

Climate Change (IPCC, 2004) concluding ‘public concerns about CO2 transportation may form a significant barrier to large-scale use of CCS’. An especially commissioned study by the US congress in April 2007 states (Order Code RL33971, 2007) ‘there are important unanswered questions about CO2 pipeline safety’. It goes on to say that ‘policy decisions affecting CO2 pipelines take on an urgency that is, perhaps, unrecognized by many’.

It is noteworthy that CO2 pipelines have been in operation in the US for over 30 year for enhanced oil recovery (Order Code RL33971, 2007). However, these are either confined to low populated areas, and/or operate below the proposed supercritical conditions (73.3 bar and 31.18 ^{o}C) that make CO2 pipeline transportation economically viable thus representing significantly less safety issues. Additionally, due to their small number, it is not possible to draw a meaningful statistical representation of the risk. The US report predicts ‘statistically, the number of incidents involving CO2 should be similar to those for natural gas transmission'. It is noteworthy that the rupture of a natural gas pipeline during the Piper Alpha tragedy (Cullen, 1990) ultimately lead to the collapse of the platform onto the sea bed, the loss of 167 lives and a cost of £2 billion.

Despite all this, UK has no standards specific to CO2 pipelines. Furthermore, CO2 is not recognised as a dangerous fluid (Encyclopaedia of Occupational Health and Safety, 1989).

The Challenge

‘A transportation infrastructure that carries carbon dioxide in large enough quantities to make a significant contribution to climate change mitigation will require a large network of pipelines spanning over hundreds of kilometres (IPCC, 2004)’. Putting this in perspective, a typical 100km, 0.8m dia. pipeline transporting CO2 at room temperature and 170bara would contain approximately 9m tons of gas.

The near adiabatic expansion process following pipeline rupture could lead to a massive and rapid release. Depending on its discharge temperature, the escaping fluid could either form a very cold jet denser than the surrounding air covering distances of several kilometres or a solid discharge with its own characteristics hazards such as delayed sublimation and impact erosion of surrounding equipment.

In both circumstances, the resulting plume is the most dangerous with regard to toxic gases due to its poor mixing with the surrounding air. Connolly and Cusco (2007) provide an excellent review of the hazards associated with the accidental release of pressurised CO2. At a concentration of 10%, an exposed individual would lapse into unconsciousness in 1minute (Lees, 1996). Furthermore, if the concentration is 20% or more, the gas is instantaneously fatal (Pohanish et al., 1996). The ability of CO2 to collect in depressions in the land, in basements and in other low-lying areas such as valleys near the pipeline route, presents a significant hazard if leaks continue undetected. Hydrocarbons will eventually ignite or explode in such areas if, and when, conditions are “right”, but CO2 can remain undetected for a very long time.

Unlike other toxic gases that operate as chemical asphyxiants, CO_2 has no choking or distinctive odour and this attribute adds to its potency as a toxic gas. In 1986 in Cameroon a cloud of naturally-occurring CO2 spontaneously released from Lake Nyos killed 1,800 people in nearby villages (Krajick, 2003).

It is clear that the hazards associated with CO2 pipelines are quite different compared to those posed by hydrocarbon pipelines, presenting a new set of challenges. As such any confidence that existing experience with operating hydrocarbon pipelines can be wholly extended to CO2 pipelines is dangerously misplaced.

Two key areas that will need to be demonstrated to gain public acceptance CO2 pipelines are that such mode of transport is safe, and its environmental impact is limited. Pivotal to this is the estimation of the flow rate and its variation with time following pipeline rupture.

In this paper we employ our previously validated CFD model, PipeTech to report and compare outflow data for the rupture of hypothetical but nevertheless realistic of two identical pressurised pipelines each containing CO2 and natural gas. Given the critical importance of the correct prediction of fluid density on the accurate prediction of outflow data, the efficacy of PipeTech in predicting CO2 densities over an extensive range of temperatures and pressures is examined first.

Background Theory

PipeTech's background theory is extensively presented in previous publications (see for example Mahgerefteh et al, 2000, Mahgerefteh et al., 2006a,b, Mahgerefteh and Abbasi, 2007). Its formulation is rigorous with its predictions having been extensively validated against available field data (see for example Mahgerefteh et al, 2006a).

Briefly, the modelling involves the numerical solution of the mass, energy and momentum conservation equations assuming 1D flow using a suitable technique such as the Method of Characteristics (MOC).

PipeTech accounts for real fluid behaviour as well as flow and phase dependent heat transfer and frictional effects. It is applicable to both isolated and un-isolated flows where pumping at the high-pressure end continues despite pipeline failure. Liquid and vapour phases are assumed to be at thermodynamic and phase equilibrium. This assumption is found to be generally valid in the case of rupture of long pipelines (Chen et al., 1995).

Peng-Robinson equation of state (Peng and Robison, 1976) coupled with appropriate mixing rules is used for obtaining the relevant thermodynamic and phase equilibrium data. The speed of sound for real multi-component single-phase fluids is obtained using standard expressions (Picard and Bishno, 1987). In the absence of an analytical solution, the speed of sound for two-phase mixtures is calculated numerically.

Results and Discussion

Applicability of PR EoS in predicting CO2 data

Although the PR EoS has been found to be particularly applicable to high-pressure hydrocarbon mixtures, its suitability in predicting CO2 properties, particularly density covering an extensive range of pressures and temperatures has not been fully investigated. This is important since the accurate prediction of the discharge rate following pipeline rupture is critically affected by the efficacy of the EoS in predicting density data.

Tables 1 -3 show the results of such analysis in the pressure and temperature range of 1 – 500 bar and 250 - 1100 K respectively. The corresponding fluid state is given in each table. The experimental data are those reported by Span and Wagner (1996). The tables also shows the predictions using the Bender EoS (Bender, 1975), specifically developed for CO2.

Based on the comparison with the experimental data in the gaseous region (tables 1 and 2), it is clear that both EoS produce remarkably good agreement with the experimental data. The maximum discrepancy produced by PR EoS is 1.9%. The corresponding value using the Bender EoS is 1.2%.

Reasonably good density predictions are also obtained in the supercritical region ((>31.9 ^{o}C and >71.9 bar; table 3) with the Bender EoS (1.7% discrepancy) performing better than the PR EoS (4.25% discrepancy).

CO2 pipeline rupture outflow data

Figures 1 - 3 show the simulated discharge data following the full bore rupture of a hypothetical 54km long and 0.419m i.d pipeline transporting pressurised CO2 at 117 bara and 283 K. For the sake of an example, these pipeline dimensions and the prevailing conditions are the same as those for the sub-sea natural gas line from Piper-Alpha to MCP-01 platform which ruptured during the Piper Alpha tragedy (Cullen, 1990). In the absence of reported values for the heat transfer coefficient, pipe wall thickness and pipe wall roughness corresponding values for a partially insulated mild steel pipeline are assumed. The corresponding simulated data for the actual natural gas inventory transported in the gas riser prior to its rupture are superimposed on the same graphs for comparison. For credibility, we chose the Piper Alpha conditions since PipeTech's output has been previously successfully validated by comparison against the actual pipeline intact end pressure data recorded during the night of the tragedy (Mahgerefteh et al, 1997).

Returning to figure 1, the data show the variation of discharge pressure with time for the first 300s following full bore pipeline rupture. Curve A shows the Piper Alpha data (natural gas). The CO2 data are presented by Curve B. As it may be observed, pipeline failure is signified by a rapid instantaneous drop from the line pressure of 117bara to 10bara in approximately 25s followed by a gradual reduction. This type of hyperbolic behaviour is synonymous with full bore rupture (Mahgerefteh et al., 2006a,b).

It is interesting to note that both the natural gas and the CO2 pipelines exhibit very similar depressurisation behaviour with the former demonstrating a marginally more rapid drop during the first 40s following rupture.

Figures 2 shows the corresponding discharge rate data for both pipelines. As it may be observed, the initial discharge rate upon rupture for the CO2 pipeline is approximately 4500 kg/s as compared to 4150 kg/s for the natural gas pipeline. Thereafter the CO2 pipeline maintains a noticeably higher discharge rate for the remainder of the discharge process under consideration.

The variation of the cumulative mass discharged with time results for the two pipelines is shown in figure 3. The data show that at any given time following rupture, a significantly larger amount of CO2 is released as compared to natural gas. Almost 260000kg of CO2 accounting for only 4% of the inventory (figure 4, curve B) escapes from the pipeline in the first 300s following rupture. Although significantly less than the amount release during the Lake Nyos irruption, nevertheless such huge amount of CO2 released in such a short period of time would lead to catastrophic consequences where it to occur in a populated area.

The corresponding mass loss for the natural gas pipeline is approximately half of this value (125000 kg) representing a much higher percentage (10 %; figure 4, curve A) of the inventory lost.

Figure 5 shows the variation of the discharge temperature with time for the CO2 pipeline. As it is clear, the initial gaseous inventory undergoes a significant drop in temperature reaching – 212K (-62^{o}C) at 4.1bara some 900s following failure corresponding to solid discharge. CO2 triple point is -56.5 ^{o}C and 5.1bara.

Conclusion

In this paper we present transient outflow predictions following the full bore rupture of a pressurised CO_2 pipeline. This data is central to assessing all the hazards associated with such type of failure.

The simulated predictions, generated using our validated CFD model, PipeTech demonstrate a hyperbolic variation in the discharge rate with time characterised by a massive amount of inventory released in a relatively short period of time following pipeline failure. This type of release behaviour is the most catastrophic, significantly limiting the emergency response time available. Comparison of the outflow data with those for the rupture of the same pipeline containing natural gas indicates a significantly greater amount of CO_2 released representing only a fraction of the initial inventory. The tracking of the temperature/pressure data of the discharged CO_2 at the rupture plane indicates cold dense vapour cloud discharge for the first 900s following rupture. This is followed by solid release at -62^{o}C and 4.1bara. The released CO_2 would cover large distances remaining at lethal concentrations for a protracted period of time prior to sublimation and dilution to safe levels.

In conclusion, the hyperbolic release behaviour characterised by the massive burst of inventory coupled with its significant cooling clearly highlight the challenges faced by safety practitioners when considering the hazards associated with the rupture of pressurised CO_2 pipelines. The type of data presented in this paper is pivotal to the quantification of such hazards.

References

Chen, J. R., S. M. Richardson, and G. Saville, 1995a, Modelling of two-phase blowdown from pipelines – I. A hyperbolic model based on variational principles, *Chem Eng Sci*, **50:** 695.

Connolly, S and Cusco, L, Hazards from high pressure carbon dioxide releases during carbon dioxide sequestration processes, Loss Prevention 2007, 12th International Symposium on Loss Prevention and Safety Promotion in the Process Industries.

Cullen, W. D., 1990, The public inquiry into the Piper Alpha disaster. *Dept of Energy*, HMSO.

Doctor, R. and Palmer, A., 2004, Transporting CO2, Chapter 4.

Encyclopaedia of Occupational Health and Safety / Technical. 3 ed., 3 impr. Geneva: International Labour Office, 1989.

Intergovernmental Panel on Climate Change, IPCC, Carbon Capture & Storage ISBN 92-9169-119.

Krajick, K., 2003, Defusing Africa's Killer Lakes. *Smithsonian*, **34(6)**: 46 – 55

Lees, F. P., 1996, Safety and Loss Prevention in the Process Industries, Hazard Identification, Assessment and Control. *Butterworth-Heinemann,* Vol. 1(15): 75, 102-104.

Lees, F. P., 1996, Safety and Loss Prevention in the Process Industries, Hazard Identification, Assessment and Control. *Butterworth-Heinemann*. Vol. 2, pp 16/87-88.

Mahgerefteh, H., Saha, P. and Economou, I., 2000, Modelling fluid phase transition effects on the dynamic behaviour of ESDV. *AIChE Journal*, **46(5):** 997 – 1006.

Mahgerefteh, H., Oke, A. and Rykov. Y., 2006a, Efficient numerical simulation for highly transient flows. *Chem Eng Sci,* **61(15):** 5049-5056.

Mahgerefteh, H., Oke, A. and Atti, O., 2006b, Modelling outflow following rupture in pipeline networks. *Chem Eng Sci*, **61(6):** 1811-1818.

Mahgerefteh, H. and Abbasi, U., 2007, Modeling blowdown of pipelines under fire attack. *AIChE Journal*, **53(9):** 2443-2450.

Mahgerefteh, H., Saha, P. and Economou, I., 1997, A study of the dynamic response of emergency shut-down valves following full bore rupture of long pipelines. *Trans I ChemE: Process Safety and Environmental Protection*, **75(B4):** 201-209

Parfomak, P. and Folger, P., 2007, Carbon Dioxide (CO2) Pipelines for Carbon Sequestration: Emerging Policy. CRS Report for Congress.

Peng, D. Y., and Robinson, D. B., 1976, A new two-constant equation of state. *Ind Eng Chem Fund*, **15:** 59-65.

Picard, D. J., and Bishnoi, P. R., 1987, Calculation of the thermodynamic sound velocity in two phase multi-component fluids. *Int J Multiphase Flow*, **13(3):** 295-308.
Span, R. and Wagner, W., **1996**, *J Phys Chem Ref Data*, **25**: 1509-1596.

Pohanish, P. R., and Greene, S.A., 1996, Hazardous Materials Handbook, Carbon Dioxide. *Van Nostrand Reinhold,* 330-331.

UK Department of Trade and Industry, 2002, Report on Carbon Dioxide Capture and Storage, *Pub URN 00/108*.

World Population Prospects: The 2002 Revision, 2003, New York: United Nations.
Cabinet Office PIU, 2002, Energy Review.

Figure legends

Figure 1. The variation of discharge pressure with time following full bore pipeline rupture
Curve A: Natural Gas (Piper Alpha)
Curve B: CO_2

Figure 2. The variation of mass release rate with time following full bore pipeline rupture
Curve A: Natural Gas (Piper Alpha)
Curve B: CO_2

Figure 3. The variation of cumulative mass discharged with time following full bore pipeline rupture
Curve A: Natural Gas (Piper Alpha)
Curve B: CO_2

Figure 4. The variation of % mass lost with time following full bore pipeline rupture
Curve A: Natural Gas (Piper Alpha)
Curve B: CO_2

Figure 5. The discharge CO_2 temperature with time following full bore pipeline rupture

Pressure (Bar)	Temperature (K)	Density (kg/m3)			% Difference	
		PR EOS	Span & Wagner (1996)	Bender EOS	PR EOS	Bender EOS
1.01325	Gas					
	250	2.165	2.165	2.164	0.02	-0.03
	300	1.798	1.797	1.796	0.06	-0.03
	350	1.538	1.537	1.537	0.04	-0.03
	400	1.344	1.343	1.343	0.03	-0.02
	450	1.194	1.193	1.193	0.03	-0.02
	500	1.074	1.074	1.073	0.02	-0.01
	600	0.894	0.894	0.894	0.02	-0.02
	700	0.766	0.766	0.766	0.02	-0.02
	800	0.670	0.670	0.670	0.01	-0.02
	900	0.596	0.596	0.596	0.01	0.11
	1000	0.536	0.536	0.536	0.01	-0.02
	1100	0.488	0.487	0.487	0.01	-0.02
	Triple point					
5	216	13.201	13.282	13.251	-0.61	-0.23
	Gas					
	250	11.109	11.097	11.093	0.11	-0.04
	300	9.068	9.046	9.044	0.25	-0.02
	350	7.690	7.674	7.671	0.21	-0.03
	400	6.688	6.677	6.675	0.16	-0.03
	450	5.923	5.915	5.913	0.13	-0.03
	500	5.318	5.313	5.311	0.11	-0.03
	600	4.421	4.417	4.416	0.09	-0.03
	700	3.784	3.781	3.781	0.07	-0.02
	800	3.309	3.307	3.306	0.07	-0.02
	900	2.940	2.938	2.938	0.06	-0.02
	1000	2.646	2.644	2.644	0.06	-0.02
	1100	2.405	2.403	2.403	0.06	-0.01

Table 1. Comparison of the performance of various equations of state in predicting CO2 densities in the gaseous state

Pressure (Bar)	Temperature (K)	Density (kg/m3)			% Difference	
		PR EOS	Span & Wagner (1996)	Bender EOS	PR EOS	Bender EOS
	Gas					
10	250	23.464	23.435	23.409	0.12	-0.11
	300	18.672	18.579	18.341	0.50	-1.28
	350	15.645	15.581	15.575	0.41	-0.04
	400	13.521	13.477	13.470	0.32	-0.05
	450	11.930	11.899	11.894	0.26	-0.04
	500	10.687	10.664	10.659	0.22	-0.05
	600	8.860	8.845	8.842	0.17	-0.03
	700	7.575	7.564	7.562	0.15	-0.02
	900	5.879	5.872	5.871	0.12	-0.01
	1000	5.289	5.283	5.282	0.12	-0.01
	1100	4.807	4.801	4.801	0.11	-0.01
50	350	91.326	89.619	89.383	1.90	-0.26
	400	73.836	72.804	72.609	1.42	-0.27
	450	63.001	62.295	62.154	1.13	-0.23
	500	55.352	54.826	54.728	0.96	-0.18
	600	44.967	44.621	44.577	0.78	-0.10
	700	38.082	37.823	37.805	0.68	-0.05
	800	33.112	32.904	32.901	0.63	-0.01
	900	29.331	29.156	29.158	0.60	0.01
	1000	26.345	26.196	26.200	0.57	0.02
	1100	23.923	23.793	23.798	0.547	0.020

Table 2. Comparison of the performance of various equations of state in predicting CO2 densities in the gaseous state

Pressure (Bar)	Temperature (K)	Density (kg/m3)			% Difference	
		PR EOS	Span & Wagner (1996)	Bender EOS	PR EOS	Bender EOS
	Super Critical					
200	400	378.302	380.500	379.813	-0.58	-0.18
	450	288.499	285.140	280.201	1.18	-1.73
	500	239.343	235.240	231.913	1.74	-1.41
	600	184.222	180.500	179.114	2.06	-0.77
	700	152.430	149.270	148.681	2.12	-0.39
	800	131.033	128.340	128.096	2.10	-0.19
	900	115.378	113.040	112.969	2.07	-0.06
	1000	103.308	101.270	101.269	2.01	0.00
	1100	93.660	91.857	91.895	1.96	0.04
500	500	548.974	534.420	539.975	2.72	1.04
	600	430.109	414.840	411.227	3.68	-0.87
	700	357.326	343.270	340.460	4.09	-0.82
	800	307.839	295.340	293.585	4.23	-0.59
	900	271.622	260.550	259.497	4.25	-0.40
	1000	243.734	233.890	233.263	4.21	-0.27
	1100	221.462	212.660	212.288	4.14	-0.18

Table 3. Comparison of the performance of various equations of state in predicting CO2 densities in the supercritical state

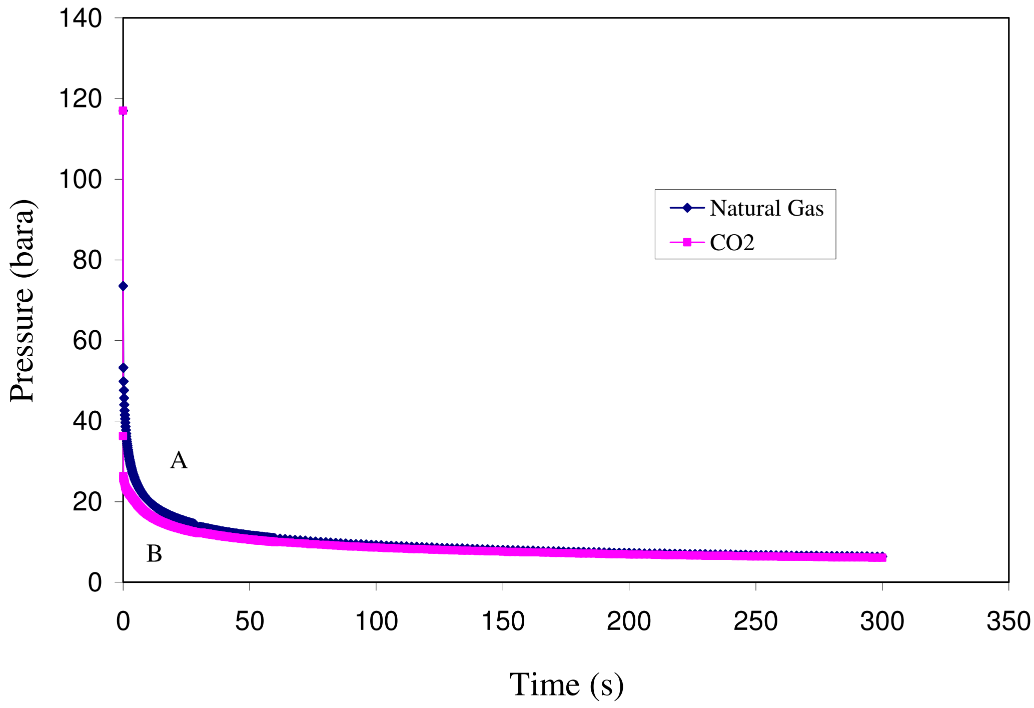

Figure 1. The variation of discharge pressure with time following full bore pipeline rupture
Curve A: Natural Gas (Piper Alpha)
Curve B: CO2

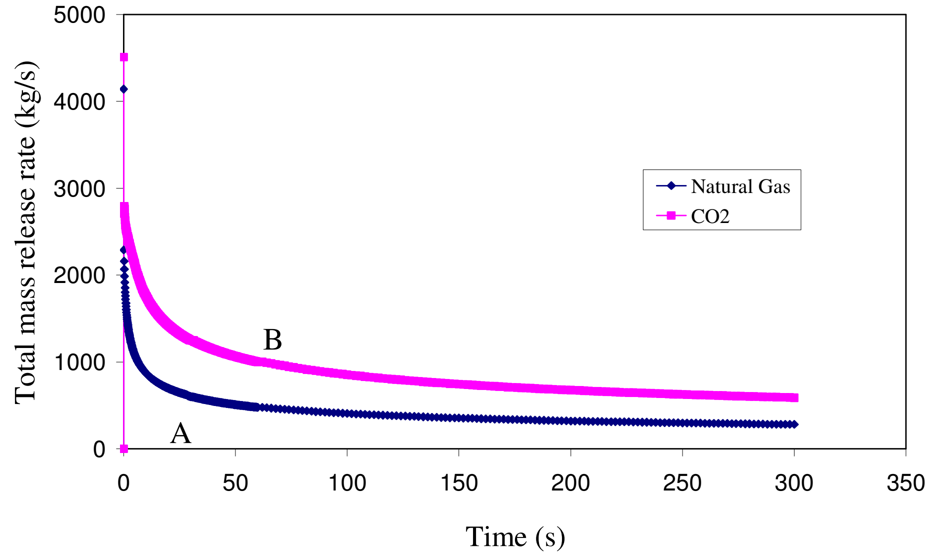

Figure 2. The variation of mass release rate with time following full bore pipeline rupture
Curve A: Natural Gas (Piper Alpha)
Curve B: CO2

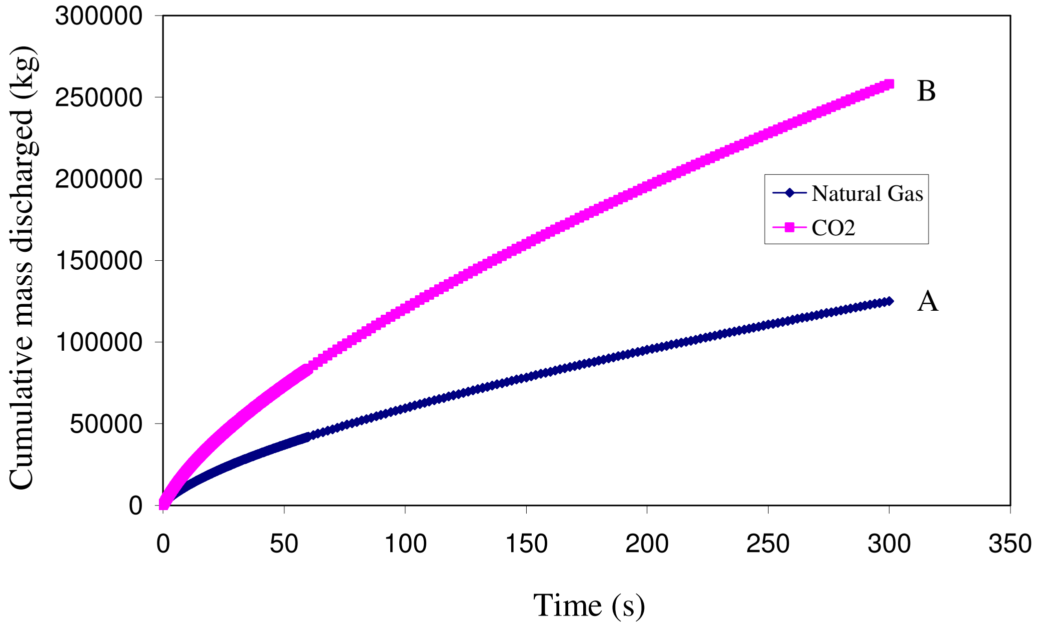

Figure 3. The variation of cumulative mass discharged with time following full bore pipeline rupture
Curve A: Natural Gas (Piper Alpha)
Curve B: CO_2

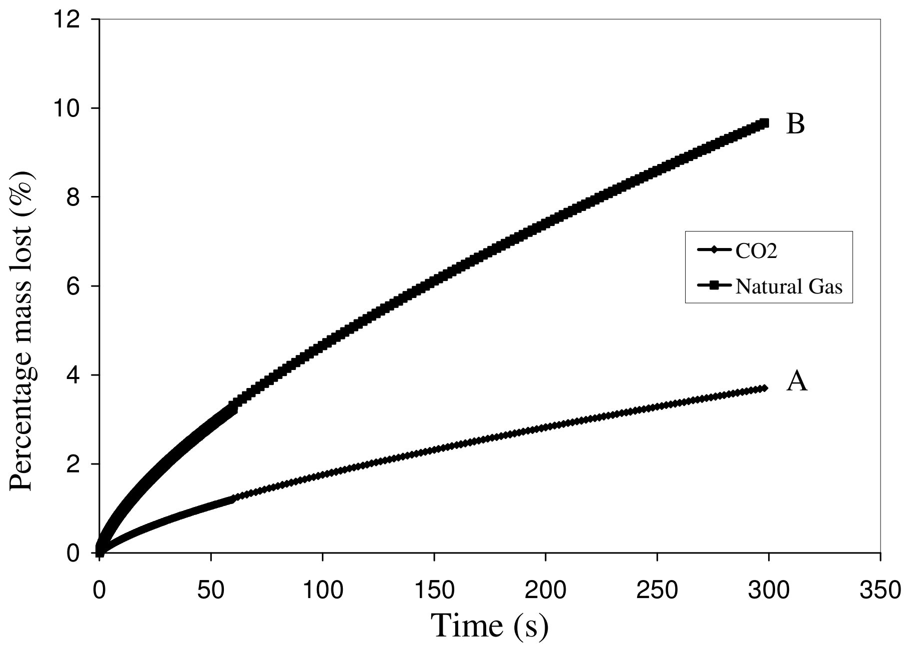

Figure 4. The variation of % mass lost with time following full bore pipeline rupture
Curve A: Natural Gas (Piper Alpha)
Curve B: CO_2

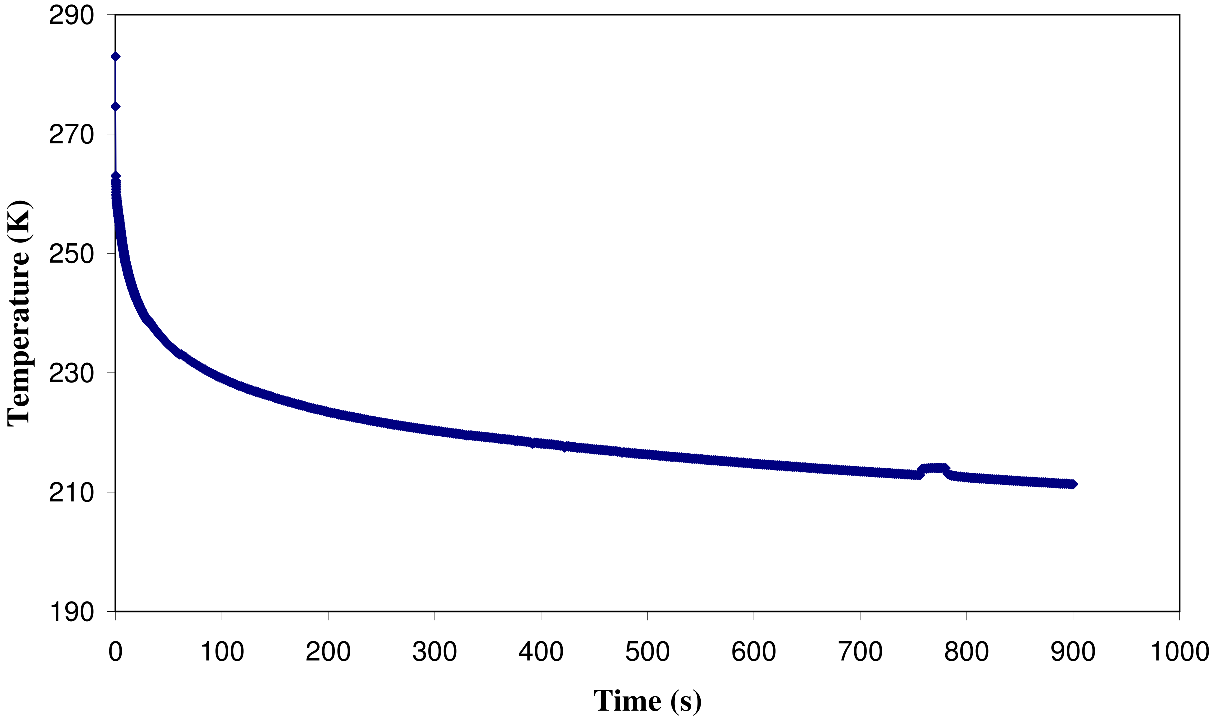

Figure 5. The discharge CO2 temperature with time following full bore pipeline rupture